Molecularly Controlled Interfacial Layer Strategy Toward Highly Efficient Simple-Structured Organic Light-Emitting Diodes

*Tae-Hee Han, Mi-Ri Choi, Seong-Hoon Woo, Sung-Yong Min, Chang-Lyoul Lee, and Tae-Woo Lee**

Organic light-emitting diodes (OLEDs) have potential applications in large area, full-colour, high resolution flat-panel displays, future flexible displays, and solid-state lighting.[1–7] Although device efficiencies and operational lifetimes of vacuum-deposited small-molecule OLEDs have been significantly increased, state-of-the-art OLED device structures have been developed to have more functional layers than did earlier OLEDs.[5–9] These functional layers facilitate charge injection, transport and blocking in the devices and thus to help balance injection and transport of holes and electrons to the emitting layer for efficient radiative recombination.[10,11] Another important role of these functional layers in multilayered OLEDs is to prevent an exciton quenching near electrodes.[12–14] The standard fabrication method for small-molecule OLEDs is vacuum deposition, which has high costs of materials and processing to fabricate multilayered structures, and so has been a critical impediment to mass production at a low cost. Therefore, achieving simple structured OLEDs while maintaining their original luminous current efficiency (*CE*) has become a major challenge that must be solved before wide industrial application of OLEDs can be economically feasible.

Emitting layers based on small molecules usually have only their own emitting function without further high charge injecting and transporting capability, so simplified small molecule OLED devices with a high *CE* have not been achieved easily unlike polymer light-emitting diodes (PLEDs) in which the single emitting polymer contains different functional (i.e. emitting, hole-transporting or electron-transporting) repeating segments.[15,16] Therefore, strategies to achieve high-*CE* OLEDs with simplified structures having a single emitting dopant/single host system should include the ways to improve (i) charge injection and transport to improve charge balance, (ii) charge blocking to increase electron-hole recombination, and (iii) block quenching of excitons to increase radiative decay. The simplification strategies in vacuum deposited OLEDs to date do not meet all the requirements at the same time.[17,18] The most critical problem to simplify the device lies on occurrence of significant exciton quenching when the recombination zone is close to the electrodes (e.g., indium tin oxides, metals or conducting polymers). Therefore, it has been very difficult to achieve high efficiency from the single-layered small molecule devices. Therefore, it would be ideal to realize efficient simplified device involving one-step vacuum deposition of a small-molecule emitting layer by removing the exciton quenching near the electrodes. In this manner, the vacuum-deposited small molecule OLEDs exploit the same simple device structure and advantages of low-cost and simple processing like the polymer light-emitting diodes to realize flexible displays and solid-state lighting devices.

This paper basically presents a fundamental and comprehensive strategy to realize very simplified small-molecule OLEDs with a very high *CE*, which include only a single emitting layer of small molecules on top of a spin-coated conducting polymer layer. Conventional conducting polymers, poly(3,4-ethylenedioxythiophene):poly(styrenesulfonate) (PEDOT:PSS) or polyaniline doped with polymeric acids have been usually used as the hole injection layer (HIL) or the anode layer;[19,20] however, in OLEDs the commonly used PEDOT:PSS has serious problems due to inefficient hole-injection, inefficient electron-blocking, and substantial quenching of excitons close to the PEDOT:PSS.[14,19,21] With simplified structures with a conventional HIL (PEDOT:PSS or a small molecule HIL), we observed a significant drop of the *CE*.

Our idea to simplify the structure to realize highly efficient small-molecule OLEDs (**Figure 1**a) uses a molecularly-controlled, high-performance interfacial polymeric HIL on the anode, which enable efficient blocking of exciton quenching as well as efficient hole-injection and efficient electron-blocking at the same time. Our HILs are composed of PEDOT:PSS and a tetrafluoroethylene-perfluoro-3,6-dioxa-4-methyl-7-octene-sulfonic acid copolymer, one of perfluorinated ionomers (PFI), which develops a gradient work function (*WF*) by self-organization of the PFI (We call "GraHIL"). This single-layered small molecule OLED has much greater *CE* (~20 cd/A) than do standard multilayered small molecule OLED devices that

T.-H. Han, M.-R. Choi, S.-H. Woo, S.-Y. Min, Prof. T.-W. Lee
Department of Materials Science and Engineering
Pohang University of Science and Technology (POSTECH)
San 31 Hyoja-dong, Nam-gu, Pohang, Gyungbuk 790-784, Korea
E-mail: twlee@postech.ac.kr
Dr. C.-L. Lee
Advanced Photonics Research Institute (APRI)
Gwangju Institute of Science & Technology (GIST)
1 Oryong-dong, Buk-gu, Gwangju, 500-712, Korea

DOI: 10.1002/adma.201104316

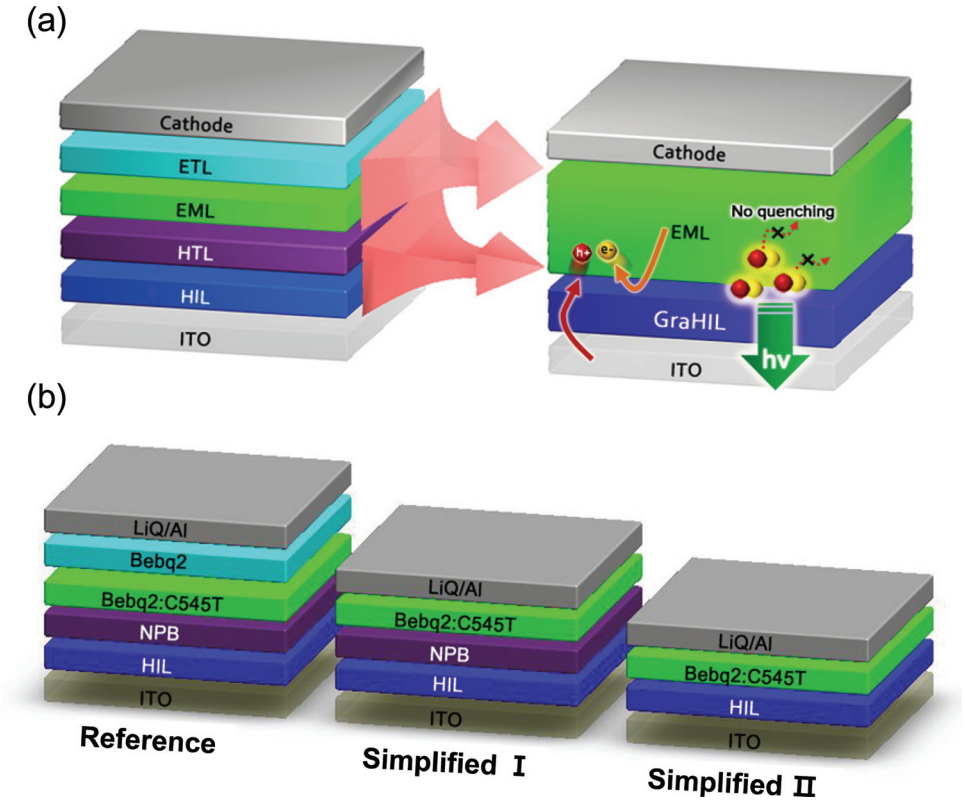

Figure 1. a) Schematics of devices conventional structures and simplified structures of OLED, b) Schematics of three different device structures of organic light emitting diodes fabricated in this experiment.

use conventional well-known hole injecting small-molecule, 4,4′,4″-tris(*N*-(2-naphthyl)-*N*-phenyl-amino)triphenylamine (2-TNATA) as a HIL (*CE* ~12 cd/A). The dramatic improvement in simplified OLEDs is achieved because that molecularly controlled GraHIL meets all the requirements for realization of simplified small-molecule OLEDs. From our studies regarding exciton quenching, we find that the self-organized surface layer of our GraHIL having efficient hole-injection/electron-blocking capability can prevent the severe quenching of excitons at the HIL/emitting layer (EML) interface without needing a hole transporting layer (HTL).

Our approach exploits a self-organized surface layer in GraHILs for blocking exciton quenching as well as improving hole injection and electron-blocking. Because fluorocarbon chains in the PFI have lower surface energy (~20 mN/m) and are more hydrophobic than PSS, PFI preferentially accumulates at the surface of GraHIL films by self-organization and the PFI concentration tends to decrease with increasing depth.(Supporting Figure S1) Also, because the PFI has higher ionization potential than the PSS,[22] the film surface with relatively higher concentrations of PFI increases the *WF*, and the concentration gradient of PFI through the HIL film forms a gradient *WF* that greatly reduces the hole injection barrier from ITO to the EML. (Supporting Table S1)

Accordingly, this polymeric HIL injects holes efficiently into the EML, and the surface-enriched PFI layer at the interface between the HIL and the EML provides great capacity to block electrons for more electron-hole recombination at the HIL/EML interface. In addition, the self-organized PFI layer on top of the PEDOT:PSS can play a role as a buffer layer to block exciton quenching caused by PEDOT:PSS.[19]

Because the GraHIL provides efficient hole injection and transport to the EML, OLED devices with GraHILs do not require an overlying HTL. As the host material of the EML, we chose bis(10-hydroxybenzo[h]quinolinato) beryllium ($Bebq_2$), a good electron transporting material with a high electron mobility.[23] In this manner, the electron transporting layer (ETL) can also be removed in our simplified devices. The holes and electrons can recombine very efficiently for radiative decay even in our simplified structure even without HTL and ETL where the recombination zone is located close to the HIL/EML interface. As a result, the fabrication process requires only one-step vacuum deposition of the EML on top of the solution processed HIL.

We have developed three OLED device structures (Figure 1b) to investigate the effect of simplification of small-molecule OLEDs on the device *CE*. The reference device has a conventional multilayered structure of ITO/HIL (50 nm)/NPB (20 nm)/$Bebq_2$:C545T (2%, 30 nm)/$Bebq_2$ (20 nm)/8-Hydroxyquinolinolato-lithium (Liq)(1 nm)/Al (130 nm). One simplified device (Type-I) without an ETL has a structure of ITO/HIL (50 nm)/NPB (20 nm)/$Bebq_2$:C545T (2%, 50 nm)/Liq (1 nm)/Al (130 nm), and the most simplified device (Type-II) without an ETL and a HTL has a structure of ITO/HIL (50 nm)/$Bebq_2$:C545T (2%, 70 nm)/Liq (1 nm)/Al (130 nm) where HILs are chosen from 2-TNATA, PEDOT:PSS (CLEVIOS P VP AI 4083, H. C. Starck GmbH), and GraHIL11.

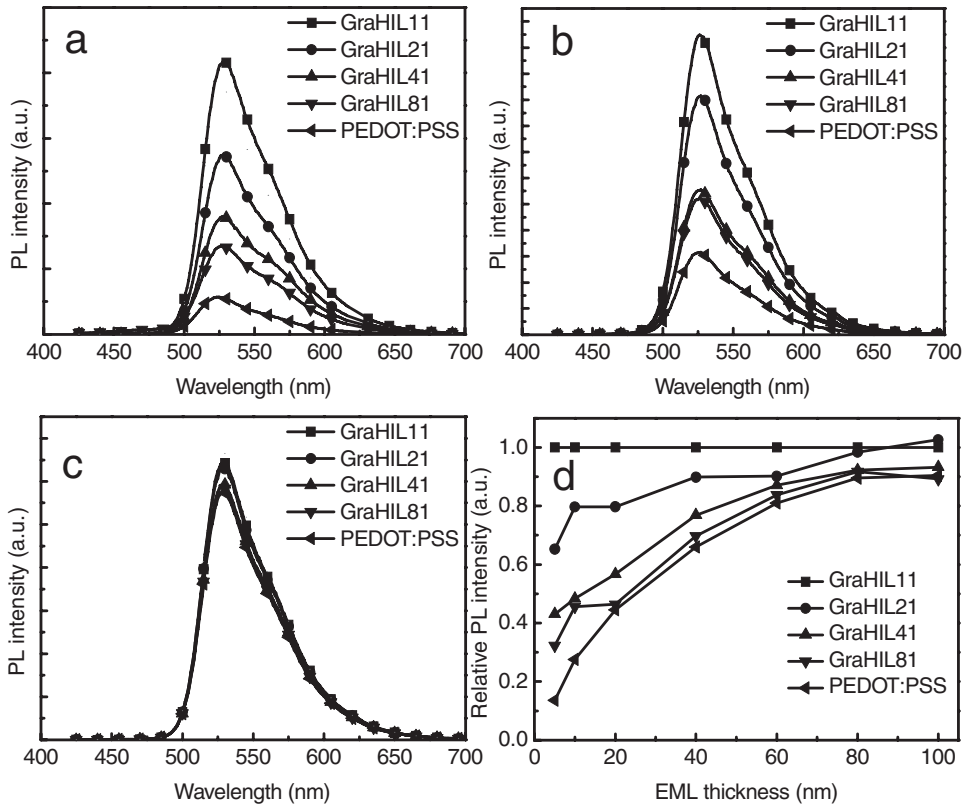

Figure 2. Photoluminescence (PL) intensities of $Bebq_2$:C545T emitting films on various hole injection layers (HILs) or substrates. PFI concentration in GraHILs: GraHIL11>GraHIL21>GraHIL41>GraHIL81, a) 5 nm-thick emitting layer, b) 10 nm-thick emitting layer, c) 80 nm-thick emitting layer, and d) normalized PL intensities on various HILs to the PL on the GraHIL11 as a function of thickness of emitting films.

To prove that the surface-enriched PFI layer helps to block exciton quenching caused by PEDOT:PSS, we measured steady state photoluminescence (PL) with various thickness of emitting layer ($Bebq_2$:C545T) and time-correlated single photon counting (TCSPC) to obtain the PL lifetime change of the thin films. The PL and TCSPC measurements were done in a sample structure of glass/PEDOT:PSS or PEDOT:PSS:PFI (GraHIL81, 41, 21 and 11, 50 nm, Supporting Table S1)/$Bebq_2$:C545T(2%) (x nm), where we varied the PFI concentration in GraHIL compositions and the thickness of the EML. PL spectra (**Figure 2**a–c) were taken for $Bebq_2$:C545T (2%) films. In samples with very thin $Bebq_2$:C545T (2%) films (x = 5, 10 nm), PL intensities from the PEDOT:PSS/$Bebq_2$:C545T films were much lower than in the GraHIL11/$Bebq_2$:C545T films; this reduction indicates larger exciton quenching by PEDOT:PSS than in the GraHIL11/$Bebq_2$:C545T films, which is most likely ascribed to two major exciton quenching mechanisms: (i) exciton dissociation (i.e. surface quenching) induced by larger band offset than the exciton binding energy[19,24] or exciton quenching induced by polaron or bipolarons in doped PEDOT[25,26] and also (ii) nonradiative energy transfer from excitons to the doped PEDOT with lower bandgap.[24] (Supporting Figure S2)

Exciton quenching was greatly reduced by using GraHILs. The PL intensities tended to increase with the relative concentration of PFI to PEDOT:PSS; this difference implies that surface-enriched PFI helps to prevent exciton quenching at the interface. Increasing the thickness of the EML caused the contrast of PL intensities among samples to decrease (Figure 2c,d), because the increased thickness means that excitons in the EML are generated far from the quenching interface and the estimated exciton diffusion length in $Bebq_2$:C545T film as short as ~10 nm (Supporting Figure S3).

TCSPC results (**Figure 3**) were consistent with the steady state PL measurements. We performed the TCSPC measurement with various samples of glass/PEDOT:PSS or GraHIL (50 nm)/$Bebq_2$:C545T (10 nm). Similarly to the steady state PL measurements, as the relative concentration of PFI in the GraHILs was increased, the PL lifetimes tended to increase gradually from 0.76 ns in the PEDOT:PSS film to 1.79 ns in the AIPF41 film and then to saturate (Figure 3b). The gradual increase of PL lifetimes implies the gradual reduction of exciton quenching at the interface between the EML and the HIL by forming a thicker self-organized surface-enriched PFI layer which keeps excitons away from the quenching interface (i.e., PEDOT:PSS) on the HIL films with higher content of PFI in the compositions.

The luminance versus voltage characteristics of the multilayered reference device with varying the HILs (**Figure 4a**) indicates that the device with GraHIL11 exhibits almost the same operating voltages to that with PEDOT:PSS and much lower operating voltages than that with 2TNATA even though GraHIL11 has a high concentration of an insulating

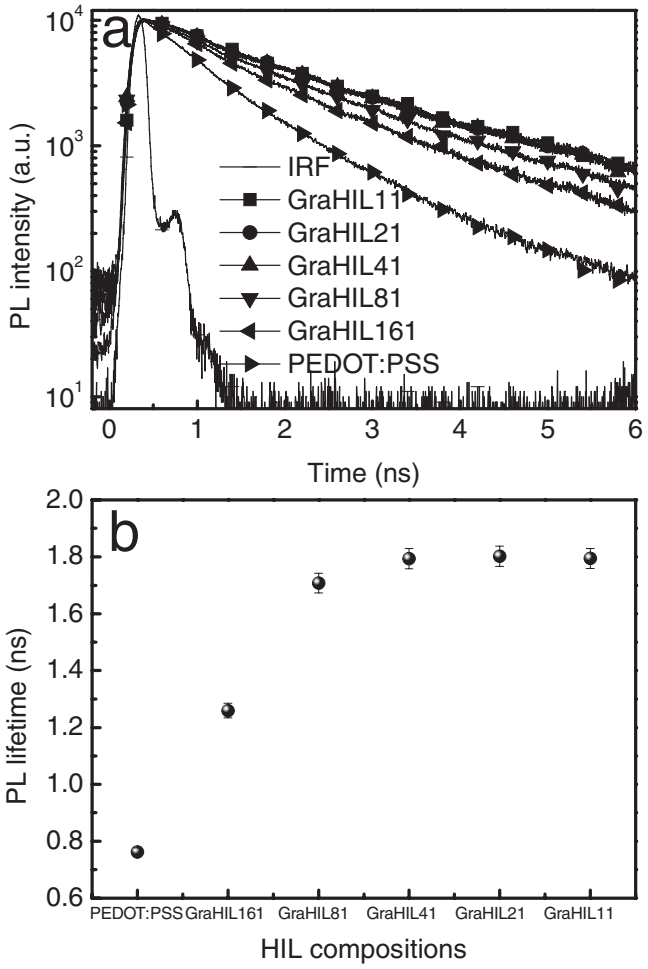

Figure 3. PL decay profiles and lifetimes of the $Bebq_2$:C545T(2%) on various hole injection layers. a) PL decay curves, b) PL lifetime obtained from time-correlated single photon counting measurement. The lifetime was monitored at 530 nm, τ_{avr} is average lifetime obtained from $f_1\tau_1 + f_2\tau_2$. (where τ_1 and τ_2 *are lifetimes (ns),* f_1 and f_2 are fractional intensities.)

component (PFI). This is consistent with the previous literature to report the effect of extra insulating PSS in PEDOT:PSS compositions on the hole injection and the *CE* in OLEDs: although film conductivity of the conducting polymer tends to decrease by increasing the insulating PSS concentration in compositions, the surface *WF* of the HILs made dominant influence on the hole injection and the *CE* rather than film conductivity.[27] Since the GraHIL has molecularly controlled gradient *WF* from bottom to the surface of the HIL, GraHIL11 can effectively reduce the injection barrier height and then facilitates the hole injection, which is supported by characterization of hole-only devices (ITO/HILs (50 nm)/NPB (300 nm)/Al (130 nm)) with GraHIL11 and conventional PEDOT:PSS (Figure 4b). The hole-only device with GraHIL11 showed much higher hole current than that with PEDOT:PSS. The *CE*-vs-voltage characteristics (Figure 4c–f) were measured for the non-simplified reference, Type-I simplified device, and Type-II simplified device with various HILs. All of the Type-I simplified devices (i.e. without an ETL) (Figure 1b) had *CEs* that were similar to those of the corresponding reference devices with no HIL (Figure 4c), 2-TNATA (Figure 4d), PEDOT:PSS (Figure 4e), and GraHIL (Figure 4f). In contrast, Type-II simplified devices with no HIL, 2-TNATA, and PEDOT:PSS (Figure 4c–e) had significantly lower *CE*s than the corresponding reference devices and the Type-I simplified devices.

The *CE* of the reference device using our GraHIL11 (~18.3 cd/A) was greater than that of the reference device that uses 2-TNATA (~12 cd/A); this improvement indicates that our polymeric HIL has excellent ability to inject holes and to block electrons. Furthermore, the *CE* of the most simplified (Type-II) structure with GraHIL11 as the HIL (~20 cd/A) is even slightly higher than those of the reference device with GraHIL11 (~18.3 cd/A) and the Type-I simplified device (16.3 cd/A). In contrast, *CEs* of Type-II simplified devices with no HIL, 2-TNATA, and PEDOT:PSS were very poor and much lower than in the device with GraHIL; this difference indicates that GraHIL has an important function in the simplified devices.

We demonstrated that most quenching of excitons occurs at the interface between HIL and EML by measuring steady state PL with various thickness of EML (Figure 2). Because $Bebq_2$ is an electron-dominant material, the recombination zone of Type-II simplified devices that lack both the HTL and the ETL, is also located at the interface between the HIL and the EML; the exciton quenching zone is the same as the recombination zone. On the other hand, the *CEs* of Type-I simplified devices were similar to those of the corresponding reference devices; this similarity indicates that the electrons can be efficiently injected from the cathode even without an ETL because of the good electron transporting capability of the host ($Bebq_2$) of the EML and the recombination zone close to NPB/EML interface is different from the exciton quenching zone.

In Type-II simplified devices, the recombination zone can be formed close to the HIL/EML interface. The absolutely low *CE* of the most simplified Type-II device using PEDOT:PSS as the HIL is due to a high hole injection barrier from the HIL to the EML, insufficient electron blocking capability, and exciton quenching at the HIL/EML interface, while the low *CE* of the Type-II device using a 2-TNATA HIL can be ascribed to inefficient hole-injection and electron-blocking at the interface. The ionization potential of 2-TNATA and PEDOT:PSS are ~5.1 eV and ~5.2 eV, which are higher than the *WF* of ITO (~4.8 eV) but hole injection barriers still occur between the HIL and the EML (~0.3–0.4 eV). Especially, in the case of the Type-II simplified device, PEDOT:PSS can significantly quench excitons at the HIL/EML interface most probably due to exciton dissociation (i.e. surface quenching) by doped PEDOT and nonradiative energy transfer from the EML to the doped PEDOT (Supporting Figure S2):[19,24–26] The exciton dissociation at the interface can be induced by (bi)polarons in oxidized PEDOT,[25,26] also by greater band offset than exciton binding energy of the EML because of the much lower acceptor level of oxidized PEDOT (–4.4 eV)[19,24] and by nonradiative energy transfer to PEDOT with a low bandgap.[24] In addition, we also find that the excitons can be quenched by PSS, judging from significant drop of photoluminescence intensity on a PSS thin film.(Supporting Figure S4) Therefore, the quenching effect at the HIL/EML interface in the Type-II simplified device using the PEDOT:PSS layer

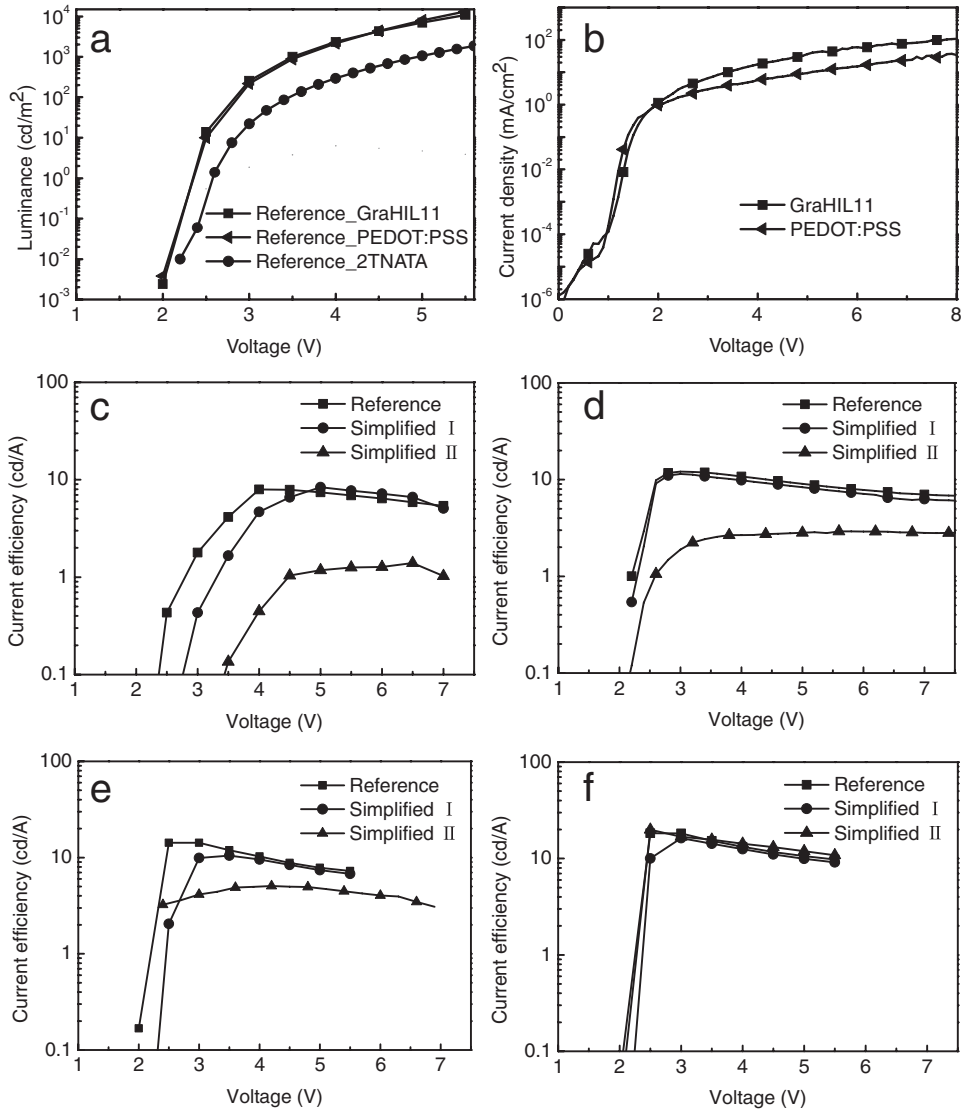

Figure 4. Luminance vs. voltage and current efficiency vs. voltage characteristics of the non-simplified and simplified OLEDs and current density vs. voltage characteristics of hole-only devices with varying hole-injection layers (HILs). a) Luminance vs. voltage characteristics of non-simplified reference devices, b) current density vs. voltage characteristics of ITO/HILs/NPB/Al hole-only devices (HIL: GraHIL11, PEDOT:PSS), c) current efficiency vs. voltage characteristics of OLED devices without hole injection layer, d) with 2TNATA, e) with PEDOT:PSS, and f) with GraHIL11 as HILs.

causes large reduction in *CE* at the low voltage regime, whereas the *CE* is further increased at the high voltage regime due to the shift of recombination zone. Therefore, we have chosen a HIL with a molecularly-controlled gradient morphology, GraHIL11, which has a high *WF* (~5.95 eV) and an insulating, surface-enriched PFI buffer layer on top of the film. The very high *CE* in the Type-II simplified structure indicates that ability to block electrons and prevent an exciton quenching was an important factor that contributed to improving the *CE* of the device with a single EML on a spin-coated polymeric GraHIL, because *CE* is related to efficient hole and electron recombination without exciton quenching at the HIL/EML interface, which is proved by steady state PL and TCSPC measurements.

The conclusive schematic drawings in the **Figure 5** helps to understand the roles of self-organized surface-enriched PFI layer in the GraHIL compositions which are capable of blocking electrons and preventing exciton quenching (Figure 5a), which results in the generation of more excitons and the more efficient radiative decay. The conventional PEDOT:PSS do not blocks electrons efficiently and thus less electron-hole recombination takes place (Figure 5b). Moreover, the generated excitons can undergo exciton quenching pathways by PEDOT:PSS layers (Figure 5b).

In conclusion, we have demonstrated an efficient simplification of the multilayered fluorescent OLED structure and achieved a high *CE* (~20 cd/A) despite the simplified structure, which consists of a single small-molecule organic EML. Even if all the simplification based on conventional HILs resulted in very poor *CE*s in the devices, a very high *CE* was observed with a spin-coated high performance polymeric GraHIL. This

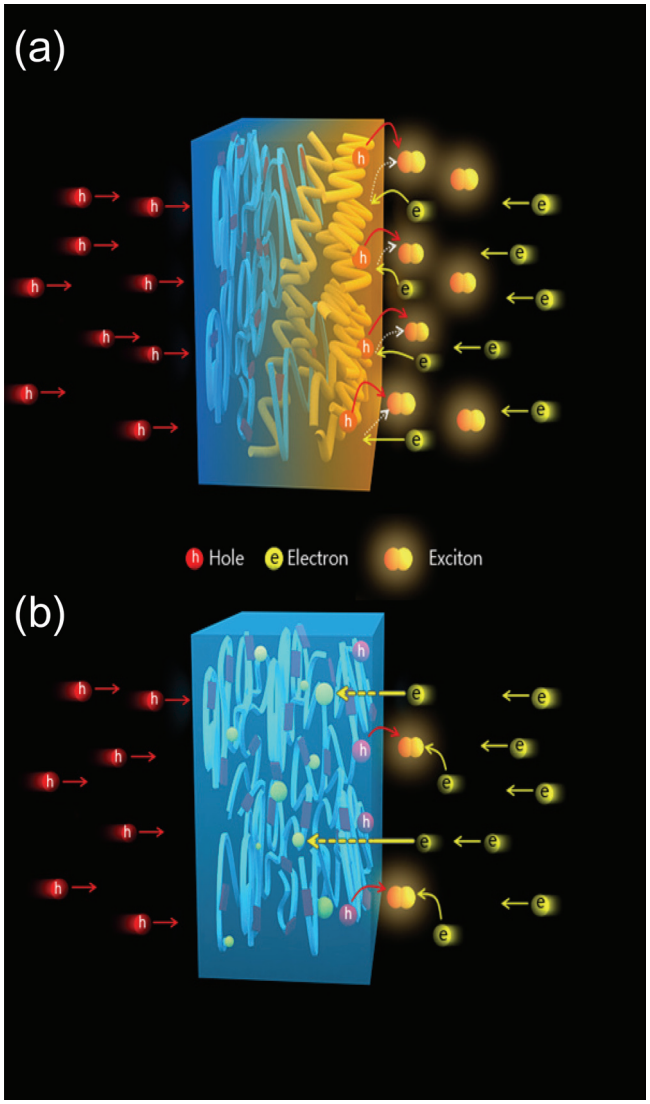

Figure 5. Schematic drawings regarding hole injection, electron-blocking, and exciton quenching depending on two different hole injection layers in OLEDs a) Schematics of self-organized PFI in hole injection layer regarding capability for injecting holes, blocking electrons and quenching of excitons, b) Schematics of quenching process of exciton dissociations by PEDOT:PSS hole injection layer.

HIL makes a gradient morphology and *WF* from the bottom to the top of the film by self-organization, and this gradient *WF* helps to achieve very efficient hole injection directly to the EML without an overlaying HTL. Furthermore, the insulating and inert character of surface-enriched PFI block electrons and exciton quenching at the HIL/EML interface where electrons and holes recombine in these simplified OLEDs. We demonstrated the gradual reduction of exciton quenching with increasing PFI content in the compositions by steady-state PL and TCSPC measurements. Therefore, holes and electrons recombine very efficiently at the interface in the simplified structure, which includes only a single-layered EML on top of the GraHIL. Our work suggests that the simplification of small molecule OLEDs should consider three key factors: (i) efficient hole injection, (ii) efficient electron-blocking, and (iii) efficient prevention of exciton quenching at the HIL/EML interface. This kind of simplification strategy with a molecularly controlled high-performance HIL is unique, not only because it will reduce the manufacturing cost related to vacuum-deposition-based OLED fabrication while maintaining the original high device *CE* in multilayered OLEDs, but also because we did not dope additional organic hole-transporting or electron-transporting compounds in the EML (i.e., single dopant doped into the single host) to facilitate hole and electron transport. Although, according to the scientific and technological roadmaps in this area to date, it has been often anticipated that the low-cost manufacturing of future flexible OLEDs would be realized in the form of PLEDs, our work suggests that low-cost manufacturing of flexible full-color OLED displays or solid-state lightings can also be realized by using simplified small-molecule devices.

Experimental Section

OLED fabrications: Indium-tin-oxide (ITO; WF ~4.8 eV) coated glasses which have square active areas of 2 × 2 mm were used as substrates for OLED fabrication. The ITO surface was UV-ozone treated for 15 min before the spin-coating or deposition of films on top of the ITO. Polymeric hole-injection layers (HILs) (PEDOT/PSS or GraHIL compositions (Supporting Information, Table S1) were spin-coated to give 50-nm films on top of the ITO/glass, then baked immediately on a hot plate in air at 200 °C for 10 min. Our GraHILs are composed of PEDOT:PSS (Clevios P VP AI4083) and a tetrafluoroethylene-perfluoro-3,6-dioxa-4-methyl-7-octene-sulfonic acid copolymer, one of perfluorinated ionomers (PFI) (CAS number: 31175-20-9) (Sigma-Aldrich Inc.). A small-molecule hole-injection layer (HIL) (2-TNATA) was vapor-deposited to achieve a 50-nm film. NPB as the hole transport layer (HTL), $Bebq_2$ as electron transport layer (ETL) or host material for emitting layer (EML), and a green-light-emitting fluorescent material C545T (2% co-deposition with $Bebq_2$) as the guest for EML were sequentially deposited following their sequences and thicknesses for their device design (Figure 1). Then, the 1-nm Liq and 130-nm Al layers were sequentially deposited on the EML or ETL. All vapor depositions were conducted under vacuum ($<5 \times 10^{-7}$ Torr). All fabricated devices in this study were sealed by glass encapsulation using a UV resin and a getter.

OLED characterization: A computer controlled source-measurement unit (Keithley 236) and a spectroradiometer (Minolta CS2000) were used to measure current-voltage-luminance (*I–V–L*) characteristics and EL spectra.

Steady-state photoluminescence (PL) measurement: The steady-state photoluminescence (PL) spectra was measured with a excitation wavelength at 415 nm by using a PL spectrometer (JASCO FP6500).

Time-Correlated Single Photon Counting measurement: For measuring PL lifetimes, time-correlated single photon counting (TCSPC) was performed. The second harmonic (SHG = 420 nm) of a tunable Ti:sapphire laser (Mira900, Coherent) with ~150 fs pulse width and 76-MHz repetition rate was used as an excitation source. The PL emission was spectrally resolved by using collection optics and a monochromator (SP-2150i, Acton). The TCSPC module (PicoHarp, PicoQuant) with an MCP-PMT (R3809U-59, Hamamatsu) was used for ultrafast detection. The total instrument response function (IRF) for PL decay was less than 150 ps, and the temporal resolution less than 10 ps. The deconvolution of actual fluorescence decay and IRF was performed using fitting software (FlouFit, PicoQuant) to deduce the time constant associated with each exponential decay.

Supporting Information

Supporting Information is available from the Wiley Online Library or from the author.

Acknowledgements

This research was supported by the Basic Research Program through the National Research Foundation of Korea (NRF), funded by the Ministry of Education, Science and Technology (Nos.2009-0090177, 2009-0075025, and 2009-0067533).

Received: November 10, 2011
Revised: December 31, 2011
Published online: February 17, 2012

[1] J. Kido, M Kimura, K. Nagai, *Science* **1995**, *267*, 1332.
[2] Z. Shen, P. E. Burrows, V. Bulovic, S. R. Forrest, M. E. Thompson, *Science* **1997**, *276*, 2009.
[3] S. R. Forrest, *Nature* **2004**, *428*, 911.
[4] G. Gu, Z. Shen, P. E. Burrows, S. R. Forrest, *Adv. Mater.* **1997**, *9*, 725.
[5] S. Reineke, F. Lindner, G. Schwartz, N. Seidler, K. Walzer, B. Lussem, K. Leo, *Nature* **2009**, *459*, 234.
[6] B. W. D'Andrade, S. R. Forrest, *Adv. Mater.* **2004**, *16*, 1585.
[7] Y. Sun, N. C. Giebink, H. Kanno, B. Ma, M. E. Thompson, S. R. Forrest, *Nature* **2006**, *440*, 908.
[8] J. Kido, T. Matsumoto, *Appl. Phys. Lett.* **1998**, *73*, 2866.
[9] X. Zhou, J. Blochwitz, M Pfeiffer, A. Nollau, T. Fritz, K. Leo, *Adv. Funct. Mater.* **2001**, *11*, 310.
[10] F. F. So, S. R. Forrest, *Phys. Rev. Lett.* **1991**, *66*, 2649.
[11] Y. Ohmori, A. Fujii, M. Uchida, C. Morishima, K. Yoshino, *Appl. Phys. Lett.* **1993**, *63*, 1871.
[12] A. L. Burin, M. A. Ratner, *J. Phys. Chem. A* **2000**, *104*, 4704.
[13] J. Mezyk, F. Meinardi, R. Tubino, M. Cocchi, *Appl. Phys. Lett.* **2008**, *93*, 093301.
[14] A. V. Dijken, A. Perro, E. A. Meulenkamp, K. Brunner, *Org. Electron.* **2003**, *4*, 131.
[15] P. K. H. Ho, J.-S. Kim, J. H. Burroughes, H. Becker, S. F. Y. Li, T. M. Brown, F. Cacialli, R. H. Friend, *Nature* **2000**, *404*, 481.
[16] D. Kabra, L. P. Lu, M. H. Song, H. J. Snaith, R. H. Friend, *Adv. Mater.* **2010**, *22*, 3194.
[17] M. G. Helander, J. Qiu, M. T. Greiner, D. P. Puzzo, Z. W. Liu, Z. H. Lu, *Science* **2011**, *332*, 944.
[18] W. S. Jeon, T. J. Park, J. J. Park, S. Y. Kim, J. Jang, J. H. Kwon, R. Pode, *Appl. Phys. Lett.* **2008**, *92*, 113311.
[19] J.-S. Kim, R. H. Friend, I. Grizzi, J. H. Burroughes, *Appl. Phys. Lett.* **2005**, *87*, 023506.
[20] a) J. E. Yoo, K. S. Lee, A. Garcia, J. Tarver, E. D. Gomez, K. Baldwin, Y. Sun, H. Meng, T.-Q. Nguyen, Y.-L. Loo, *Proc. Nat. Acad. Sci.* **2010**, *107*, 5712; b) M.-R. Choi, S.-H. Woo, T.-H. Han, K.-G. Lim, S.-Y. Min, W. M. Yun, O. K. Kwon, C. E. Park, K.-D. Kim, H.-K. Shin, M.-S. Kim, T. Noh, J. H. Park, K.-H. Shin, J. Jang, T.-W. Lee, *ChemSusChem* **2011**, *4*, 363.
[21] H. Yan, B. J. Scott, Q. Huang, T. J. Marks, *Adv. Mater.* **2004**, *16*, 1948.
[22] a) T.-W. Lee, Y. Chung, O. Kwon, J.-J. Park, *Adv. Funct. Mater.* **2007**, *17*, 390; b) M.-R. Choi, T.-H. Han, K.-G. Lim, S.-H. Woo, D. H. Huh, T.-W. Lee, *Angew. Chem. Int. Ed.* **2011**, *50*, 6274; c) T.-H. Han, Y. Lee, M.-R. Choi, S.-H. Woo, S.-H. Bae, B. H. Hong, J.-H. Ahn, T.-W. Lee, *Nat. Photon.* **2012**, *6*, 105.
[23] J.-H. Lee, S. W. Liu, C.-A. Huang, K. H. Yang, Y. Cha, *Proc. SPIE* **2004**, *5464*, 434.
[24] J. Mei, M. S. Bradley, V. Bulović, *Phys. Rev. B* **2009**, *79*, 235205.
[25] S. Hayashi, S. Kaneto, K. Yoshino, *Solid State Commun.* **1987**, *61*, 249.
[26] J. C. Bolinger, M. C. Traub, T. Adachi, P. Barbara, *Science* **2011**, *331*, 565.
[27] T.-W. Lee, Y. Chung, *Adv. Funct. Mater.* **2008**, *18*, 2246.